J Exp Biol Advance Online Articles. First posted online on 4 March 2016 as doi:10.1242/jeb.124081
Access the most recent version at http://jeb.biologists.org/lookup/doi/10.1242/jeb.124081

Morphology and motion: hindlimb proportions and swing phase kinematics in terrestrially locomoting charadriiform birds

Brandon M. Kilbourne[†1,2,3], Emanuel Andrada[1], Martin S. Fischer[1], John A. Nyakatura[1,4,5]

[1]Institut für Spezielle Zoologie und Evolutionsbiologie, Friedrich-Schiller-Universität Jena, Erbertstraße 1, 00743 Jena, Germany

[2]College for Life Sciences, Wissenschaftskolleg zu Berlin, Wallotstraße 19, 14193 Berlin, Germany

[3]Museum für Naturkunde Berlin, Invalidenstraße 43, 10115 Berlin, Germany

[4]Image Knowledge Gestaltung—an Interdisciplinary Laboratory, Humboldt-Universität zu Berlin, Unter den Linden 6, 10099 Berlin, Germany

[5]Institute of Biology, Humboldt-Universität zu Berlin, Philippstraße 13, 10115 Berlin, Germany

[†]Corresponding author: brandon.kilbourne@mfn-berlin.de

Journal of Experimental Biology • Advance article

Summary: Differing limb proportions in terms of length and mass, as well as differences in mass being concentrated proximally or distally, influence the limb's moment of inertia (MOI), which represents its resistance to being swung. Limb morphology—including limb segment proportions—thus likely has direct relevance for the metabolic cost of swinging the limb during locomotion. However, it remains largely unexplored how differences in limb proportions influence limb kinematics during swing phase. To test whether differences in limb proportions are associated with differences in swing phase kinematics, we collected hindlimb kinematic data from three species of charadriiform birds differing widely in their hindlimb proportions: lapwings, oystercatchers, and avocets. Using these three species, we tested for differences in maximum joint flexion, maximum joint extension, and range of motion (RoM), in addition to differences in maximum segment angular velocity and excursion. We found that the taxa with greater limb MOI—oystercatchers and avocets—flex their limbs more than lapwings. However, we found no consistent differences in joint extension and RoM among species. Likewise, we found no consistent differences in limb segment angular velocity and excursion, indicating that differences in limb inertia in these three avian species do not necessarily underlie the rate or extent of limb segment movements. The observed increased limb flexion among these taxa with distally heavy limbs resulted in reduced MOI of the limb when compared to a neutral pose. A trade-off between exerting force to actively flex the limb and potential savings by a reduction of MOI is skewed towards reducing the limb's MOI due to MOI being in part a function of the radius of gyration squared. Increased limb flexion likely is a means to lower the cost of swinging the limbs.

Key Words: Limbs; Proportions; Locomotion; Kinematics; Charadriiformes; Moment of Inertia

Introduction

Since the early 1900s functional anatomists have proposed that limb morphology reflects the locomotor capacity of tetrapods. Taxa with more lightweight and distally light legs should possess lower locomotor costs and may attain higher speeds (Lull, 1904; Gregory, 1912; Howell, 1944; Smith & Savage, 1956; Gray, 1968; Gambaryan, 1974; Hildebrand, 1984, 1985, 1988; Hildebrand & Hurley, 1985; Steudel, 1990; Wickler et al., 2004; Raichlen, 2005, 2006; Browning et al., 2007). In contrast, taxa with more massive and distally heavy legs should incur higher locomotor costs or might be restricted to slower speeds of terrestrial locomotion (e.g., Kilbourne & Hoffman, 2013). Limbs with greater and more distal concentrations of mass should have higher moments of inertia (MOI) – an increased resistance to angular acceleration or, more simply, to swinging the limb back and forth (Steudel, 1990; Wickler et al., 2004; Kilbourne & Hoffman, 2013, 2015). This constitutes a link between morphology and locomotor capacity. Thus, limb MOI reflects morphological characteristics (overall limb mass and its distribution) that should directly influence the energetic costs of the limb's swing phase during locomotion.

How exactly differences in limb morphology relate to limb kinematics—particularly swing phase kinematics—has been little explored. Dissimilar proportions of segment lengths curtail the range of kinematics that species can employ during terrestrial locomotion, resulting in dissimilar excursion angles of individual segments due to geometric constraints (Pike & Alexander, 2002; Gatesy & Pollard, 2011). Given the same angular excursion in the proximal joint, a longer segment will displace the distal end of the segment further. Differences in the proportions of segment masses and the overall mass distribution of the limb may affect the motions of the limb during swing phase (Hildebrand & Hurley, 1985; Wickler et al., 2004; Nelson & Roberts, 2008). Distal limb segments with a high mass result in a longer radius of gyration and, consequently, a greater limb MOI (e.g., Kilbourne, 2014). However, reducing the radius of gyration *via* kinematic adjustments (e.g., more pronounced flexion) during swing phase is a means to reduce limb MOI.

Birds are one of the largest tetrapod lineages and represent an impressive range of hindlimb functions and specializations, making them an ideal group in which to study how limb morphology influences locomotor capability, particularly in terms of kinematics (Abourachid and Höfling, 2012). Within Aves, the Charadriiformes—or the shorebird clade—comprise one of the major avian clades (Hackett et al., 2008;

Jetz et al., 2012), encompassing a diversity of differing hindlimb proportions (Barbosa and Moreno, 1999). The combination of close phylogenetic affinity and high limb morphological diversity makes Charadriiformes a group well suited to study how length and mass proportions are reflected in hindlimb swing phase kinematics as predicted by the above considerations of limb MOI.

In the present study, we will test for differences in hindlimb swing phase kinematics among three species of charadriiform birds differing in their hindlimb morphology: northern lapwings (*Vanellus vanellus*), Eurasian oystercatchers (*Haematopus ostralegus*), and pied avocets (*Recurvirostra avosetta*) (Fig. 1). Segmental mass and length data were available for one specimen per species: lapwings have relatively short limbs (152.6 mm anatomical hindlimb length) with a low mass (hindlimb mass 10.75 g), whereas oystercatchers have only moderately longer limbs (172.8 mm), but with a much higher mass (31.38 g). In contrast, avocets possess relatively lightweight limbs (16.94 g) that are, however, elongate and slender (225.7 mm). Moreover, avocets have a distal concentration of limb mass (Kilbourne, 2013; Fig. 1).

By studying these three closely related species of differing limb segment proportions and limb mass distribution, we will test whether differences in limb morphology are associated with differences in hindlimb kinematics reflecting adjustments to reduce MOI. Additionally, we will derive the hindlimb's MOI of representative swing phases using *in vivo* kinematic data to compare these data to the hindlimb MOI of the previously published 'neutral pose' (this pose is determined by manually extending the limbs to their maximum length and then releasing the limb to passively flex on its own accord; data from Kilbourne, 2013).

Our sample allows the comparison and discussion of two specific test cases: (1) Similar limb segment proportions, but different 'neutral pose' MOI. Lapwings and oystercatchers have similar limb segment proportions, but a stark difference in 'neutral pose' MOI due to the overall higher limb mass in the oystercatcher. For similar limb flexion, animals with overall more massive but otherwise similar limbs (e.g., in terms of limb segment proportions) should exhibit greater swing durations, as increasing mass itself also increases limb MOI (Kilbourne, 2013; Kilbourne & Hoffman, 2013). (2) Similar 'neutral pose' MOI, but different limb segment proportions. Oystercatchers and avocets display similar 'neutral pose' MOI due to the distal concentration of limb mass in the avocet; however, these species possess highly

different limb segment proportions. Species with distally heavy limbs are expected to display relatively longer swing phase durations (Nelson & Roberts, 2008). Flexing their limbs is a means for birds with distally heavy limbs, such as the avocets of our sample, to effectively achieve a reduction of the limb's MOI.

Material & Methods

Study animals. Four individuals of avocet, oystercatcher, and lapwing each were obtained from a local breeder approved by Friedrich-Schiller-Universität Jena (Table 1). All animals were legally bred and ringed in 2010 and 2011. When not performing in experiments, the animals were kept in the animal house of the Institute for Systematic Zoology and Evolutionary Biology with access to food and water *ad libitum*. During experiments the birds were given ample opportunities for rest and had free access to water when not on the treadmill. Animal husbandry and all experimentation with the birds followed animal welfare regulations of the state of Thuringia, Germany and were approved by the responsible authorities (registry number: 02-47/10).

Experimental design. Cineradiographic videos were recorded for each bird locomoting on a treadmill using a fully digital Neurostar fluoroscope, (Siemens AG, Erlangen, Germany). To prevent the birds from flying away from the treadmill, a Plexiglas enclosure was placed atop the treadmill. At the rear end of the treadmill prior to where the belt passes under the carriage, a softly padded surface was placed so as to avoid injury to the birds.

Videos were recorded at 1,000 Hz for each bird in lateral view. The digital image for each frame possessed a resolution of 1,536 x 1,024 pixels, and the x-ray source for the fluoroscope operated at 40 kV and 95 mA. Cineradiographic recordings suffer from typical fluoroscope distortion (e.g., Brainerd et al., 2010). Therefore, prior to digitization of skeletal landmarks, cineradiographic videos were undistorted using a MATLAB (The MathWorks Inc., Natick, MA, USA) routine (www.xromm.org) that is one of the freely available tools as part of the X-ray Reconstruction Of Moving Morphology technique developed at Brown University, RI, USA (for details see Brainerd et al., 2010). We selected for analysis only trials in which a bird's torso was in full view in the front of the image intensifier.

Data analysis. From each video, the following skeletal landmarks were digitized: the cranial extreme of the pelvis and the proximal and distal ends of the

femora, tibiotarsi, and tarsometatarsi (Fig. 2). The distal extreme of digit III was also digitized; however, this landmark often went in and out of the camera image during the stride cycle, preventing the inclusion of this landmark during data analysis. From the skeletal landmarks, the angles of the hip, knee, and intertarsal ("ankle") joints were calculated throughout the entire swing phase. For each joint, minimum and maximum joint angles and ranges of motion (RoM) were determined for each stride's swing phase using custom written code in R version 2.15.1 (R Core Development Team, 2012). For the thigh, shank, and pes, we also calculated the maximum excursion of these segments during swing phase by obtaining the angle the segment swings through about its proximal pivot. With this, we calculated the angular velocity of the thigh, shank, and pes by means of the second derivative of joint angles using the R package pspline (Ramsey, 2013). Stride frequency, duty factor, and stance and swing durations were also determined.

Statistics. For each of the three species, maximum and minimum joint angles and RoM, stride frequency, duty factor and stance and swing durations were plotted against both absolute and dimensionless speed. The relationship between each parameter and speed was then fitted with linear and power functions. These two functions were chosen given their prevalence in describing relationships between biological traits, and for their ease of facilitating comparisons across species. To determine the function that best fit our data, we calculated corrected Akaike Information Criterion (AICc) scores (Akaike, 1973, 1974; Hurvich & Tsai, 1989) using the R package qpcR (Speiss, 2014). When a given trait was best fit by the same curve type (e.g., a power function) across more than one species, 95% confidence intervals for regression parameters (e.g., intercept, slope, etc.) were compared to determine if those species differ in their relationships between the above locomotor parameters and speed.

To further determine if the three species differ in their kinematics, we compared the maximum and minimum joint angles and RoM within specific speed ranges to investigate how limb flexion varies between the differing species. Minimum joint angles represent maximum flexion, whereas maximum joint angles represent maximum extension. To parse out any effect of speed, we only examined joint angles over ranges of absolute (0.0-1.70 m/s) or dimensionless speeds (0.0-1.32) shared by all species. We then divided these common speed ranges into three categories of low, medium, and high speeds. For absolute speed, low, medium, and high categories

respectively ranged from 0.0-0.56 m/s, 0.56-1.13 m/s, and 1.13-1.70 m/s. For dimensionless speeds, low, medium, and high categories respectively ranged from 0.0-0.44, 0.44-0.88, and 0.88-1.32. For Using a Kruskal-Wallis test, we tested for significant differences in joint maximum and minimum angles and RoM between species for each speed interval. For the Kruskal-Wallis test, the independent factor corresponded to the differing species. Our level of significance was $P < 0.05$; however, after applying a Bonferroni correction to account for our comparison of three species, $P_{significant} < 0.0167$. Post-hoc tests were used to compare individual species. Kruskal-Wallis tests and their associated post-hoc tests were performed in R, using the packages pgirmess (Giraudoux, 2015) and coin (Hothorn et al., 2006, 2008).

It should be noted that we used both absolute and dimensionless speeds for our analysis. Dimensionless speed, which is the square root of the Froude number, standardizes absolute speed to hip height using the equation: $\hat{u} = u[gh]^{-0.5}$. Standardizing to hip height minimizes differences in hip height as a confounding factor in the different ranges of locomotor speed exhibited by locomoting tetrapods (Gatesy & Biewener, 1991). Also, as the Froude number represents the ratio of inertial to gravitational forces (Raichlen et al., 2013), dimensionless speed may also be an indicator of this ratio of forces. However, an implicit assumption in using dimensionless speed is that the effect of size is ostensibly consistent across all morphological and locomotor traits – the 'larger' species will have a greater body mass and hip height and use a higher range of speeds (for an example, see the species compared in Gatesy & Biewener, 1991). Moreover, this assumption is explicit with regards to Froude number as proposed by Alexander & Jayes (1983), though the authors argue for the metric's utility even if this assumption is not strictly followed. In light of this, we also analyzed our data using absolute speed. Absolute speed arguably is the most important metric of speed with regards to how animals function in their environment, especially as it relates to prey capture and predator avoidance or the movements of herds composed of different ontogenetic stages of one species and/or species of differing sizes. While the focus of our study is not ecology, including absolute speed as a variable in our study may allow future studies to address how morphology and locomotor performance relate to animals functioning in their natural environment and allow for inferences as to why species of differing morphologies and locomotor abilities may or may not co-exist in particular habitats.

Estimation of hindlimb MOI. One individual of each species was euthanized and dissected (Table 1). Hindlimb elements were detached at the joints and frozen. We then weighed each element and used a pendulum method to determine each element's CoM position (Table 2; Nyakatura et al., 2012). We also measured segment lengths using calipers. We used these data to model each hindlimb segment as a three-dimensional geometric solid using the CAD-software Inventor®. Femur and tibiotarsus were modelled as truncated elliptic cones, while tarsometatarsus and digits were modelled as cylinders. From these solids we estimated the MOI of each segment (J_i) about its CoM (Table 2). The moment of inertia of each segment with respect to the hip was then computed frame by frame based on the parallel-axis formula: $J_i^{hip} = J_i + m_i s_i$; where m_i is the mass of the segment and s_i the distance between each segment's CoM and the hip. Finally, the sum of these segmental MOI $\sum_{i=1}^{n} J_i^{hip}$ yields the MOI of the limb with respect to the hip.

Results

To determine significant differences among species in how a given temporal parameter varies with speed, we used 95% confidence intervals to compare parameters of fit curves (e.g., the exponent *b* of a power function). For Kruskal-Wallis tests comparing among species differences in joint kinematics and segment excursions and angular velocity, our level of significance was $P < 0.05$; however, after applying a Bonferroni correction to account for our comparison of three species, our level of significance became $P_{significant} < 0.0167$.

Temporal kinematic traits

All three species largely overlap in plots of temporal kinematic traits vs. speed (Figs. 3 and S1), with the variation of stride frequency, duty factor, swing duration, and stance duration with increasing speed being best described by a power function (Table S1). While analyses involving absolute and dimensionless speed differ in values of parameters (Table 3), the overall results do not differ between the uses of these two measures of speed. It is worth noting that the difference in AICc scores is seemingly trivial between linear and power fits for some temporal parameters (e.g., swing duration in avocets, Table S1). Significant differences among all three charadriiform species exist with regards to how stride frequency varies with speed

(Table 3). Lapwings tend to utilize higher stride frequencies at lower speeds than oystercatchers, though both species converge upon similar stride frequencies with increasing speed. Compared to these two species, avocets shallowly increase stride frequency with increasing speed.

Duty factor decreases with increasing speed in a largely parallel manner among all three species (Figs. 3B and S1B), though significant differences exist among the species (Table 3). However, note that lapwings tend to use overall lower duty factors than the remaining two species (Figs. 3B and S1B).

In spite of being largely invariant with speed in all three species (Figs. 3C and S1C), swing duration minimally (but nonetheless significantly) varies with speed in lapwings and oystercatchers (Table 3), while it does not in avocets. At higher speeds, avocets tend to employ slightly higher swing durations than the other two charadriiforms, owing to their higher constant *a* (Table 3).

Avocets tend to use significantly higher stance durations than the remaining two charadriiforms (Figs. 3D and S1D; Table 3). Lapwings and avocets do not significantly differ in the exponents of their power functions (parameter *b*, Table 3); however, these two taxa do differ in their constant (parameter *a*). These results indicate that although lapwings and avocets vary their stance duration with speed in indistinguishable ways, the absolute values of their stance durations differ. Oystercatchers differ from these two species in both coefficient *a* and exponent *b*.

Limb Flexion Traits

The overall kinematic pattern during swing phase is very similar in the three analyzed species (Fig. S2). Across all absolute speed categories, oystercatchers and avocets flex their hips more than do lapwings, whereas lapwings extend their hips more than the other species (Fig. 4). Posthoc tests indicate that maximal hip flexion significantly differs among all three species ($P < 0.0167$). Likewise, maximal hip extension also significantly differs among all three species ($P < 0.0167$) across the three speed categories. Hip RoM significantly differs among the species ($P < 0.0001$; Fig. 4C), though the difference is not significant difference between avocets and oystercatchers at low speeds ($P > 0.0167$). These results do not change when using dimensionless speeds to define our three speed categories (Fig. S3).

Across all absolute speed categories, maximum knee flexion significantly differs amongst all three charadriiforms ($P < 0.0167$). Posthoc tests reveal that

lapwings flex their knees less than the other two charadriiforms ($P < 0.0167$; Fig. 4D), whereas the difference between avocets and oystercatchers is not significant at low and medium speeds ($P > 0.0167$). Differences in knee maximal extension are significant ($P < 0.0167$; Fig. 4E). Avocets have a lower maximal knee extension compared to the remaining two species across all speed categories ($P < 0.0167$). In contrast, lapwings and oystercatchers do not differ in maximal knee extension within any speed category ($P > 0.0167$). Knee RoM differs among the species for all speed categories ($P < 0.0167$), though posthoc tests reveal that only oystercatchers and lapwings consistently differ across all speed categories ($P < 0.0167$), with lapwings having a smaller knee RoM (Fig. 4F). When using speed categories defined by dimensionless speeds, the only change in results is that knee RoM does not differ between lapwings and avocets for low and medium speed categories (Fig. S3; $P > 0.0167$).

Across all absolute speeds, maximal intertarsal joint flexion significantly differs among the three species ($P < 0.0167$); however, the only consistent difference across speed categories is significantly greater flexion in oystercatchers compared to the other two species ($P < 0.0167$; Fig. 4G). Across all speeds, maximal intertarsal joint extension significantly differs between lapwings and the other two charadriiforms ($P < 0.0167$; Fig. 4H), while avocets and oystercatchers do not differ in maximal intertarsal joint extension for any speed category ($P > 0.0167$). Intertarsal joint RoM significantly differs between oystercatchers and the other two charadriiforms across all speed ranges ($P < 0.0167$; Fig. 4I), with the exception that oystercatchers and lapwing not significantly differing within the high-speed range ($P > 0.0167$). Differences in intertarsal joint RoM do not differ between avocets and lapwings for any speed range ($P > 0.0167$). At low and medium dimensionless speeds, maximum flexion significantly differs among all three species, though the differences between avocets and lapwings are not significant at high dimensionless speeds (Fig. S3; $P > 0.0167$). Across all dimensionless speed categories, maximum intertarsal extension is significantly greater in lapwings than in avocets and oystercatchers. Differences in RoM among species when using dimensionless speeds mirror those found when using absolute speeds.

Segmental velocity and excursion traits

At low absolute speeds, thigh maximum angular velocity does not significantly differ among the three species ($P > 0.0167$; Fig. 5A). Significant differences do occur at both medium and high absolute speeds ($P < 0.0167$). This is solely due to avocets having a significantly lower velocity than the other two species ($P < 0.0167$), as the difference between lapwings and oystercatchers is not significant at medium and high speeds ($P > 0.0167$). Across all dimensionless speed categories, significant differences are present among species, with oystercatchers having higher thigh angular velocities at low speeds than the remaining two species ($P < 0.0167$; Fig. S4). However, as when using absolute speeds, avocets exhibit significantly lower thigh angular velocities than oystercatchers and the lapwings ($P < 0.0167$).

Thigh angular excursion tends to increase more gradually with speed in avocets than in lapwings or oystercatchers (Fig. 5B). Thigh angular excursion does not significantly differ among the three species at low absolute speeds ($P > 0.0167$; Fig. 4B); though this trait significantly differs among all species at medium and high speeds ($P < 0.0167$). Across all dimensionless speed categories, significant differences exist among species (Fig. S4; $P < 0.0167$), with avocets having significantly lower excursion angles than lapwings (all speeds) and oystercatchers (only medium and high speeds). At high speeds, lapwings and oystercatchers also significantly differ in thigh angular excursion ($P < 0.0167$).

Oystercatchers tend to employ greater shank angular velocities than either avocets or lapwings (Fig. 5C), and shank angular velocity differs among the three charadriiforms across all three absolute speed categories ($P < 0.0167$). Posthoc tests indeed reveal that oystercatchers have greater shank angular velocities than the remaining two species across all speed categories ($P < 0.0167$). At low and medium speeds, angular velocity does not significantly differ between lapwings and avocets ($P > 0.0167$). Across all dimensionless speed categories, oystercatchers have a significantly higher shank angular velocity than the remaining two species (Fig. S4; $P < 0.0167$). However, significant differences among all three species were only found at low dimensionless speeds ($P < 0.0167$).

Shank angular excursion significantly differs among individual species with the exception of avocets and lapwings at high speeds ($P < 0.0167$; Figs. 5D and S4D),

regardless of whether absolute or dimensionless speeds are used to define speed categories.

Pes angular velocity differs among the three species for all absolute speed categories ($P < 0.0167$, Fig. 5E). However, at low speeds, the difference between avocets and lapwings is not significant ($P > 0.0167$); however, within the remaining speed categories, the differences among all three species are significant ($P < 0.0167$). Notably oystercatchers have a higher pes angular velocity across the entire analyzed speed range. Across all dimensionless speeds, oystercatchers have significantly higher pes angular velocities than avocets and lapwings (Fig. S4E; $P < 0.0167$); however, the difference between avocets and lapwings is only significant at high speeds ($P < 0.0167$).

Pes angular excursion significantly differs among the three species for all absolute speed categories ($P < 0.0167$; Fig. 5F). However, the only consistent difference across speed categories is that the pes excursion of oystercatchers is higher than that of avocets. Only at low and high dimensionless speeds, we found differences in pes angular excursion. At low dimensionless speeds, oystercatchers have a significantly higher pes angular excursion than avocets and lapwings ($P < 0.0167$; Fig. S4F), whereas at high dimensionless speeds, avocets have a significantly lower pes angular excursion than lapwings and oystercatchers ($P < 0.0167$).

Discussion

Temporal traits

Among the three species, lapwings and oystercatchers tend to use higher stride frequencies than avocets, particularly at moderate and high speeds (Fig. 3). An important factor influencing stride frequency is limb length (Gatesy and Biewener, 1991). It therefore is not surprising that the species with the overall shortest limbs uses the highest frequency, whereas the species with the longest limbs displays the lowest frequency. With the lapwings and oystercatchers, two species can be compared that have similar limb segment proportions and overall length, but highly different limb MOI (test case 1). In contrast to our expectation, both species displayed highly similar swing phase durations. The short swing phase displayed by lapwings can likely be explained by the low overall rotational inertia of their hindlimbs. However, the similarly short swing phase durations of oystercatchers are likely due to more massive joint flexors and extensors, which may afford them an ability to rapidly

accelerate their limbs (see discussion below). In particular, as the knee is the primary pivot of the hindlimb (Gatesy, 1990, 1999a,b; Gatesy and Biewener, 1991; Carrano, 1998; Reilly, 2000; Stoessel & Fischer, 2012), the greater shank segmental velocities (Fig. 5) of oystercatchers may enable their short swing phase durations (though note that the hip's contribution to hindlimb kinematics increases with increasing speeds [Gatesy, 1999a; Nyakatura et al., 2012; Stoessel & Fischer, 2012; Andrada et al., 2013]). Moreover, oystercatchers displayed overall larger segment excursions than the lapwings, which resulted in higher segment velocities given the similar swing duration in both species. Our expectations were met in regard to test case 2 (similar MOI, but different limb segment proportions). Avocets with their relatively more slender and elongate, but distally heavy segments (Fig. 1) use longer swing durations, as they have a high hindlimb rotational inertia (Kilbourne, 2013) and likely a relatively low amount of muscle mass to accelerate and decelerate the hindlimb.

Across absolute and dimensionless speeds, the largely invariant swing phase durations of the three charadriiforms agree with previous studies which have found this trait to be nearly constant with increasing speed during terrestrial locomotion of birds (Gatesy, 1999a; Reilly, 2000; Verstappen et al., 2000; Abourachid, 2001; van Coppenolle & Aerts, 2004; Rubenson et al., 2004; White et al., 2008; Nudds et al., 2010; Nyakatura et al., 2012; Stoessel & Fischer, 2012). The cost of swinging the limbs has been directly measured as being 26% of the total metabolic energy expended in running guinea fowl (Marsh et al., 2004), the invariant swing durations with increasing speed suggests that birds are limited in being able to more rapidly swing their limbs and thus rotational inertia of swinging limbs may be an important limiting factor in terrestrial locomotion (also see Rocha-Barbosa et al., 2005; Kilbourne, 2013; Kilbourne & Hoffman, 2013, 2015).

Larger bodied birds tend to increase their velocity through increases in stride length as opposed to increases in stride frequency, whereas the converse is true in small-bodied birds (Gatesy & Biewener, 1991). Muscle fiber area (which serves as a proxy for muscle force) scales isometrically with body mass (Maloiy et al., 1979; Bennett, 1996), resulting in large-bodied birds having muscles that produce less force relative to their body mass than small-bodied birds, as, under isometric scaling, body mass is proportional to length^3. In contrast, muscle fiber area is proportional to length^2 under isometric scaling. As limb MOI is known to scale either with isometry (Maloiy et al., 1979) or positive allometry (Kilbourne, 2013), and limb and segment masses

are known to scale with positive allometry (Kilbourne, 2013, 2014), large-bodied birds in general may be severely hampered in swinging their limbs more rapidly, as these traits all scale with exponents much higher than 1.0. As an allometric exponent of 2/3 characterizes how muscle fiber area scales with increasing body size under isometric scaling, the discrepancies between exponent values of 2/3 and those greater 1.0 indicate that limb MOI and segment masses increase disproportionately in comparison to the force of muscles as birds increase in size.

Joint flexion

Recent studies have found (Marsh et al., 2004; Doke et al., 2005; Arellano & Kram, 2014) or estimated (Pontzer, 2007; Umberger, 2010) the cost of swinging the limbs to be nontrivial. However, this still leaves the majority of locomotor costs to be due to stance phase. It remains poorly understood as to whether tetrapods employ mechanisms or actions to lower their limb MOI and consequently reduce the amount of torque required, which would result in lower swing phase costs. Our findings indicate that increased limb flexion is likely a means to lower swing phase locomotor costs in taxa with limbs that have greater overall mass or are distally heavier. Increased flexion of the limb brings the mass of the distal limb segments closer to the limb's pivot, thereby reducing the limb's MOI (due to a reduction in the radius of gyration) and thus the torque and, consequently, the metabolic energy required to swing it. More pronounced hindlimb flexion in the avocets and oystercatchers (Fig. 4) results in a larger reduction of rotational inertia in comparison to the more extended limbs of lapwings. Thus with regards to test case 1, oystercatchers showed more pronounced flexion than lapwings even though limb proportions and relative distribution of mass is similar in both species. With regards to test case 2, our expectation was met: avocets with relatively heavier distal limbs segments flexed the hip and knee (though not the intertarsal joint) the most during swing. For species with distally heavy limbs the benefits of flexion should be the largest. Pronounced limb flexion is used regardless of whether the greater MOI is due to greater mass (e.g., oystercatchers) or a longer radius of gyration (e.g., avocets) (Fig. 1).

Displaying MOI over the duration of swing phase in representative trials reveals the close link to the swing phase joint kinematics (Fig. 6). Flexion of the limb joints shortens the radius of gyration and thus the MOI. When the limb is extended in preparation of the subsequent stance phase the limb's MOI is increased almost to or

even above the level of the 'neutral pose' MOI (Kilbourne, 2013). This increase of MOI may also help to slow down protraction at the end of swing.

Segment angular velocity

In spite of our findings regarding joint flexion, we found no consistent response among the three charadriiforms regarding limb segment angular velocity. Oystercatchers tend to exert higher angular velocities on their shank and pedal segments than the remaining two species, though these differences are not always significant (Figs. 5 and S4). Thus, it appears that greater limb segment masses do not limit the ability to swing the limb segments at higher speeds. This result contradicts the implications of scaling and suggests that oystercatchers deviate from the expected trend (see discussion above; Kilbourne, 2013). A possible explanation for the high angular velocities observed in this species is that the greater mass of the hindlimb segments in oystercatchers (Fig. 1) is due at least in part to greater muscle mass. This apparently enables them to partly offset detrimental scaling effects. Our finding that oystercatchers tend to have higher segment angular velocities when using dimensionless speeds to partition speed categories further underscores this possibility. Given that dimensionless speeds are meant to mitigate the influence of size upon locomotor velocities observed for different species, the higher angular velocities of oystercatchers is unlikely to be purely a consequence of differences in body size.

A greater muscle mass distributed across joint flexors and extensors is likely linked to greater force production and postural/joint stability and would allow oystercatchers to better accelerate their hindlimb segments and attain greater segmental velocities. Estimates of segment soft tissue mass – which should largely reflect differences in muscle mass – in our three sampled species give credence to the possibility that oystercatchers have a greater hindlimb muscle mass than avocets and lapwings (Table 4). Given that oystercatchers locomote over a similar range of absolute velocities as lapwings in spite of their greater body masses (Figs. 1 and 3), it seems likely that they may need greater hindlimb extensor mass to accelerate their more massive bodies to a similar speed.

Greater segment masses being due to greater muscle masses underscores that overall limb morphology may be intimately tied to both swing and stance phase kinematics, and, as such, there may be a trade-off in morphological design between swing and stance phase performance. Such a trade-off has been noted several times in

tetrapods, in particular with regards to minimizing the mass of the distal limb segments through digit reduction and/or a concentration of limb mass proximally along the limb (Howell, 1944; Gray, 1968; Coombs, 1978; Hildebrand, 1988; Alexander, 1997; Pasi & Carrier, 2003; Kemp et al., 2005). A concentration of mass towards the limb's proximal end offers greater out-lever velocities (*via* more proximal muscle insertions) and lower limb rotational inertia and is therefore advantageous for swing phase. Conversely, proximal mass concentration and proximal muscle insertions offer less leverage to muscles for torque production and postural stability (i.e., mechanical advantage) during stance (Gray, 1968; Biewener, 1989). It should also be noted that morphology advantageous for greater swing phase economy might compromise limb function not only for stance phase but also for other functions, such as digging and swimming. Digging and swimming, as well as prey subdual, rely upon more distal muscle insertions along the limb for increased mechanical advantage and consequently a more distal concentration of muscle mass (Smith & Savage, 1956; Pasi & Carrier, 2003; Moore et al., 2013; Kilbourne & Hoffman, 2015).

Does inertia necessitate flexion?

Does increased limb inertia necessarily entail greater flexion? Unfortunately, the majority of studies conducting multi-species comparisons of kinematics has focused on stance phase and/or has not considered limb inertia. An exception to this, Ren et al. (2008) measured the limb kinematics of African and Asian elephants and compared them to previously published data on other mammals. They found that in spite of being graviportal and their reputation for 'columnar' limbs, elephants use RoMs during swing phase similar to other, smaller mammals. While similarity in RoM does not necessarily entail similarity in maximum limb flexion, it does suggest such a similarity is plausible. Thus, differences in limb segment proportions and limb mass distribution may not necessarily entail differences in limb flexion.

On the one hand, flexing the limbs more strongly, so as to draw the mass of distal limb segments closer to the limb's pivot, would decrease the radius of gyration of the limb and reduce its MOI, resulting in the limb requiring less energy to swing forward (Wickler et al., 2004). On the other hand, limb flexion during swing phase in birds seems to be achieved in large parts by active muscle shortening (especially the M. iliotibialis cranialis and M. iliotibialis lateralis pars preacetabularis; cf. Gatesy, 1999b) with a yet unresolved role of passive mechanisms. Thus, excessively flexing

the limbs during swing phase is likely also connected to additional muscle work and costs, and thus an optimum probably exists for the degree of limb flexion during swing. Intriguingly, swing phase duration in many mammals and birds seems to be highly invariant intraspecifically and often hardly changes with speed (e.g., Gatesy and Biewener, 1991; Abourachid, 2001; Fischer et al., 2002; Stoessel and Fischer, 2012). Potentially this reflects that animals operate closely to an optimum in the trade-off between saving energy by reducing a limb's MOI and spending extra energy to achieve this. Interspecifically however, morphological differences can be expected to be reflected in different degrees of limb flexion and temporal swing phase characteristics. Distally heavy limbs are most expensive to flex, but flexing distally heavy limbs also offers the largest benefit in terms of reducing MOI. The work to flex the limb is proportional to the product of force (i.e., mass) and distance, whereas the MOI is proportional to the product of mass and the square of distance (i.e., [the radius of gyration]$^{2.0}$). Clearly, this trade-off is likely to be skewed towards reducing the radius of gyration, given that this distance is squared.

To gain insight into how differences in limb mass and mass distribution influence the metabolic energy consumed during locomotion, Taylor et al. (1974) monitored oxygen consumption in cheetahs, gazelles, and goats—three taxa similar in body mass yet different in limb mass and its distribution—locomoting over a similar range of speeds. Surprisingly, they found that differences in oxygen consumption (a direct measure of energy expenditure) were negligible among the three species. One possible reason for minimal differences in locomotor costs among these taxa might be differences in flexion of the limbs (not measured by Taylor et al., 1974), with the more distally heavy limbs of the cheetah being flexed more in comparison to species with more distally light limbs (i.e., kinematic adjustments that influence the MOI during swing).

In the current study, the increased flexion of the hindlimbs during swing phase as a means to reduce MOI and consequently the cost of swing phase is explored. But do other mechanisms exist? One possible mechanism explored in previous studies—though unexplored in birds—is protraction of the limb through elastic energy storage (Taylor et al., 1980). Elastic energy storage has been proposed for the mammalian forelimb in the tendon of the M. biceps brachii (Wilson et al., 2003, Lichtwark et al., 2009) and also for the epaxial muscles (Alexander et al., 1985). However, these mechanisms obviously benefit quadrupeds not bipeds. Elastic energy storage has also

been proposed for the tensor fascia latae of the mammalian hindlimb (Bennett, 1989). In these mechanisms muscles and their associated fascia and tendons undergo substantial stretching during stance phase. In addition to limb protraction, the stretching of such elastic tissues during late stance may also aid to flex more distal limb joints during the start of swing phase. Therefore, other means of elastic energy storage should be investigated in birds, ideally alongside measurements of locomotor costs. For example in the ostrich—the largest living biped capable of endurance runs at high velocities—a passive engage-disengage-mechanism has been identified and has been shown to contribute to rapid intertarsal flexion and extension during swing phase (Schaller et al., 2009).

To conclude, when compared to a 'neutral pose' expected and observed flexing of the limb during swing phase in three species of morphologically diverse shorebirds was demonstrated to result in a reduced MOI throughout most of swing phase. This mechanism likely presents a way to lower the metabolic costs of swinging the limb, since a trade-off between investing additional muscle work to flex the limb and the potential reward *via* a reduction of the limb's MOI should be skewed towards reducing MOI due to MOI being a function of the square of the radius of gyration.

Acknowledgements

We would like to thank Ingrid Weiß and Rommy Petersohn for their expertise and technical assistance in collecting cineradiographic footage. We would also like to thank Irina Mischewski, Patricia Henze, Itziar Candeal, and Marc Thomsen for their diligence in digitizing cineradiographic videos, and Yefta Sutedja, Ben Derwel, and Anvar Jakupov for their help in estimating the segmental MOIs. We would also like to thank Sylke Frahnert and Pascal Eckhoff for additional access to skeletal specimens. Alexander Stößel helped to design this study. Anonymous reviews improved the clarity of previous versions of this manuscript.

Funding

This project was supported by a grant from the Deutsche Forschungsgemeinschaft (Grant No. Fi 410/15-1).

Author Contributions

B. M. Kilbourne: Design of experiments, data collection and analysis, manuscript preparation and revision (including text and figures), supervision of student work.

E. Andrada: Measurement of limb segment properties, calculation of MOI data, manuscript revision.

M. S. Fischer: Writing grant proposal, design of experiments, selection of species, and supervision of student work.

J. A. Nyakatura: Design of experiments, specimen acquisition, data collection and analysis, manuscript preparation and revision (including text and figures), supervision of student work.

The authors declare no competing interests.

References

Abourachid, A. (2001). Kinematic parameters of terrestrial locomotion in cursorial (ratites), swimming (ducks), and striding birds (quail and guinea fowl). *Comp. Biochem. Physiol. A* **131**, 1139-119.

Abourachid, A, and Höfling, E. (2012). The legs: a key to bird evolutionary success. *J. Ornithol.* **153**, 193-198.

Akaike, H. (1973). Information theory as an extension of the maximum likelihood principle. In *Second International symposium on information theory* (ed. B.N. Petrov and F. Csaki), pp. 267-281.Budapest: Akademiai Kiado.

Akaike, H. (1974). A new look at the statistical model identification. *IEEE Trans. Automatic Control* **19**, 716–723.

Alexander, R.M. (1977). Terrestrial Locomotion. *In Mechanics and Energetics of Animal Locomotion* (ed. R.M. Alexander and G. Goldspink), 168-203. London: Chapman & Hall.

Alexander, R.M. (1997). A theory of mixed chains applied to safety factors in biological systems. *J. Theor. Biol.* **184**, 247-252.

Alexander, R.M., Dimery, N.J., and Ker, R.F. (1985). Elastic structures in the back and their role in galloping in some mammals. *J. Zool.* 207, 467-482.

Alexander, R.M. and Jayes, A.S. (1983). A dynamic similarity hypothesis for the gaits of quadrupedal mammals. *J. Zool.* **201**, 135-152.

Andrada, E., Nyakatura, J.A., Bergmann, F., and Blickhan, R. (2013). Adjustments of global and local hindlimb properties during terrestrial locomotion of the common quail (*Coturnis coturnix*). *J. Exp. Biol.* **216**, 3906-3916.

Arellano, C.J. and Kram, R. (2014). Partitioning the metabolic cost of human running: a task-by-task approach. *Integr. Comp. Biol.* **54**, 1984-1098.

Barbosa, A. and Moreno, E. (1999). Hindlimb morphology and locomotor performance in waders: an evolutionary approach. Biol. J. Linn. Soc. **67**, 313–330.

Bennett, M.B. (1996). Allometry of the leg muscles of birds. *J. Zool.* **238**, 435-444.

Bennett, M.B., Ker, R.F., Alexander, R.M. (1989). Elastic strain energy storage in the feet of running monkeys. *J. Zool.* **217**, 469-475.

Biewener, A.A. (1989). Scaling body support in mammals: limb posture and muscle mechanics. *Science* 245, 45-48.

Brainerd, E.L., Baier, D.B., Gatesy, S.M., Hedrick, T.L., Metzger, K.A., Gilbert, S.L., and Crisco, J.J. (2010). X-ray reconstruction of moving morphology (XROMM): precision, accuracy, and applications in comparative biomechanics research. *J. Exp. Zool.* **313A**, 262-279.

Browning, R.C., Modica, J.R., Kram, R., and Goswami, A. (2007). The effects of added mass of the legs on the energtics and biomechaincs of walking. *Med. Sci. Sports. Exerc*. **39**, 515-525.

Carrano, M.T. (1998). Locomotion in non-avian dinosaurs: integrating data from hindlimb kinematics, in vivo strains, and bone morphology. *Paleobiol* **24**, 450-469.

Coombs, W.P. Jr. (1978). Theoretical aspects of cursorial adaptations in dinosaurs. *Quart. Rev. Biol.* 53, 393-418.

Doke, J., Donelan, J.M., and Kuo, A.D. (2005). Mechanics and energetics of swinging the human leg. *J. Exp. Biol.* **208**, 439-445.

Fischer, M.S., Schilling, N., Schmidt, M., Haarhaus, D., and Witte, H. (2002). Basic limb kinematics of small therian mammals. *J. Exp. Biol.* **205**, 1315-1338.

Gambaryan, P.P. (1974). How Mammals Run: Anatomical Adaptations (trans. by H. Hardin). New York: Wiley.

Gatesy, S.M. (1990). Caudofemoral musculature and the evolution of theropod locomotion. *Paleobiol.* **16**, 170-186.

Gatesy, S.M. (1999a). Guineafowl hindlimb function. I: cineradiographic analysis and speed effects. *J. Morph.* **240**, 115-125.

Gatesy, S.M. (1999b). Guineafowl hindlimb function. II: electromyograhic analysis and motor pattern evolution. *J. Morph.* **240**, 127-142.

Gatesy, S.M. and Biewener, A.A. (1991). Bipedal locomotion: effects of speed, size and limb posture in birds and humans. *J. Zool.* **224**, 127-147.

Gatesy, S.M. and Pollard, N.S. (2011). Apples, oranges, and angles: comparative kinematic analysis of disparate limbs. *J. Theor. Biol*. **282**, 7-13.

Giradoux, P. (2015). pgirmess: data analysis in ecology. R package version 1.6.2. http://CRAN.R-project.org/package=pgirmess.

Gray, J. (1968). *Animal Locomotion*. New York: Norton Press.

Gregory, W.K. (1912). Notes on the principles of quadrupedal locomotion and on the mechanism of the limbs in hoofed animals. *Ann. N.Y Acad. Sci.* **22**, 267-294.

Hackett, S.J., Kimball, R.T., Reddy, S.R., Bowie, R.C.K., Braun, E.L., Braun, M.J., Chojnowski, J.L., Cox, W.A., Han, K.-L., Harshman J. et al. (2008). A phylogenomic study of birds reveals their evolutionary history. *Science* **320**, 1763-1768.

Hildebrand, M. (1984). Rotations of the leg segments of three fast-running cursors and an elephant. *J. Mamm*. **65**, 718-720.

Hildebrand, M. (1985). Walking and running. In *Functional Vertebrate Morphology* (ed. M. Hildebrand, D.M. Bramble K.F. Liem, and D.B. Wake), pp. 38–57. Cambridge: Belknap Press.

Hildebrand, M. (1988). Form and function in vertebrate feeding and locomotion. *Amer. Zool*. **28**, 727-738.

Hildebrand, M. and Hurley, J.P. (1985). Energy of the oscillating legs of a fast-moving cheetah, pronghorn, jackrabbit, and elephant. *J. Morph*. **184**, 23-31.

Hothorn, T., Hornik, K., van de Weil, M.A., and Zeileis, A. (2006). A lego system for conditional inference. *Amer. Statist*. **60**, 257-263.

Hothorn, T., Hornik, K., van de Wiel, M.A., and Zeileis, A. (2008). Implementing a Class of Permutation Tests: The coin Package. *J. Stat. Softw.* **28,** 1-23.

Howell, A.B. (1944). *Speed in Animals: Their Specializations for Running and Leaping*. Chicago: University of Chicago Press.

Hurvich, C.M. and Tsai C.L. (1989). Regression and time series model selection in small samples. *Biometrika* **76**, 297-307.

Jetz, W., Thomas, G.H., Joy, J.B., Hartmann, K., and Mooers, A.O. (2012). The global diversity of birds in space and time. *Nature* **491**, 444-448.

Kemp, T.J., Bachus K.N., Nairn, J.A., and Carrier, D.R. (2005). Functional trade-offs in the limb bones of dogs selected for running versus fighting. *J. Exp. Biol.* **208**, 3475-3482.

Kilbourne, B.M. (2013). On birds: scale effects in the neognath hindlimb and differences in the gross morphology of wings and hindlimbs. *Biol. J. Linn. Soc*. **110**, 14-31.

Kilbourne, B.M. (2014). Scale effects and morphological diversification in hindlimb segment mass proportions in neognath birds. *Front. Zool.* **11**, 37.

Kilbourne, B.M. and Hoffman, L.C. (2013). Scale effects between body size and limb design in quadrupedal mammals. *PLoS ONE* **8**, e78392.

Kilbourne, B.M. and Hoffman, L.C. (2015). Energetic benefits and adaptations in mammalian limbs: scale effects and selective pressures. *Evolution* **69**, 1546-1559.

Lichtwark, G.A, Watson, J.C., Mavrommatis, S., and Wilson, A.M. (2009). Intensity of activation and timing of deactivation modulate elastic energy storage and release in a pennate muscle and account for gait-specific initiation of limb protraction in the horse. *J. Exp. Biol.* **212**, 2454-2463.

Lull, R.S. (1904). Adaptations to aquatic, arboreal, fossorial, and cursorial habits in mammals. IV. Cursorial adaptations. *Amer. Nat.* **38**, 1-11.

Maloiy, G.M.O., Alexander, R.M., Njau, R., and Jayes, A.S. (1979). Allometry of the legs of running birds. *J. Zool.* **187**, 161-167.

Marsh, R.L., Ellerby D.J., Carr, J.A., Henry, H.T., and Buchanan, C.I. (2004). Partitioning the energetics of walking and running: swinging the limbs is expensive. *Science* **303**, 80-83.

Moore, A.L., Budny, J.E., Russell, A.P., and Butcher, M.T. (2013). Architectural specialization of the intrinsic thoracic limb musculature of the American badger (*Taxidea taxus*). *J. Morph.* 274, 35-48.

Nelson, F.E. and Roberts, T.J. (2008). Task-dependent force sharing between muscle synergists during locomotion in turkeys. *J. Exp. Biol*. **211**, 1211-1220.

Nudds, R.L., Gardiner, J.D., Tickle, P.G., and Codd, J.R. (2010). Energetics and kinematics of walking in the barnacle goose (*Branta leucopsis*). *Comp. Biochem. Physiol. A* **156**, 318-324.

Nyakatura, J.A., Andrada, E., Grimm, N., Weise, H., and Fischer, M.S. (2012). Kinematics and center of mass mechanics during terrestrial locomotion in northern lapwings (*Vanellus vanellus*, Charadriiformes). *J. Exp. Zool*. A **317**, 580-594.

Pasi, B.M. and Carrier, D.R. (2003). Functional trade-offs in the limb muscles of dogs selected for running vs. fighting. *J. Evol. Biol.* **18**, 324-332.

Pike, A.V.L. and Alexander, R.M. (2002). The relationship between limb

segment proportions and joint kinematics for the hind limbs of quadrupedal mammals. *J. Zool*. **258**, 427-433.

Pontzer, H. (2007). Predicting energy cost of terrestrial locomotion: a test of the LiMb model in humans and quadrupeds. *J. Exp. Biol.* **210**, 484-494.

R Development Core Team. (2014). R: a language and environment for statistical computing. Vienna: R Foundation for Statistical Computing. ISBN 3-900051-07-0. Available at: http://www.R-project.org; 2014.

Raichlen, D.A. (2005). Ontogeny of limb mass distribution in infant baboons (*Papio cynocephalus*). *J. Hum. Evol.* 49, 452-467.

Raichlen, D.A. (2006). Effect of limb mass distribution on mechanical power outputs during quadrupedalism. *J. Exp. Biol.* **209**, 633-644.

Raichlen, D.A., Pontzer, H., and Shapiro, L.J. (2013). A new look at the dynamic similarity hypothesis: the importance of swing phase. *Biol. Open* **0**: 1-5.

Ramsey, J. (2015). pspline: Penalized Smoothing Splines. R package version 1.0-16. http://CRAN.R-project.org/package=pspline. R port by Ripley, B.

Reilly, S.M. (2000). Locomotion in the quail (*Coturnix japonica*): the kinematics of walking with increasing speed. *J. Morph.* **243**, 173-185.

Ren, L., Butler, M., Miller, C., Paxton, H., Schwerda, D., Fischer, M.S., and Hutchinson, J.R. (2008). The movements of limb segments and joints during locomotion in African and Asian elephants. *J. Exp. Biol.* **211**, 2735-2751.

Rocha-Barbosa, O., de Castro Loguercio, M.F., Renous, S., and Gasc, J.-P. (2005). Limb joint kinematics and their relation to increasing speed in the guinea pig *Cavia porcellus* (Mammalia: Rodentia). *J. Zool.* **266**, 293-305.

Rubenson, J., Heliams, D.B., Lloyd, D.G., and Fournier, P.A. (2004). Gait selection in the ostrich: mechanical and metabolic characteristics of walking and running with and without an aerial phase. *Proc. R. Soc. B* **27**, 1091-1099.

Schaller, N.U., Herkner, B., Villa, R., and Aerts, P. (2009). The intertarsal joint of the ostrich (*Struthio camelus*): anatomical examination and function of passive structures in locomotion. *J. Anat.* **214**, 830-847.

Smith, J.M. and Savage R.J.G. (1956). Some locomotory adaptations in mammals. *Zool. J. Linn. Soc.* **42**, 603-622.

Speiss, A.-J. (2014). qpcR: modelling and analysis of real-time PCR data. R package version 1.4-0. http://CRAN.R-project.org/package=qpcR

Steudel, K. (1990). The work and energetic cost of locomotion. I. The effects of

limb mass distribution in quadrupeds. *J. Exp. Biol.* **154**, 273-285.

Stoessel, A., and Fischer, M.S. (2012). Comparative intralimb coordination in avian bipedal locomotion. *J. Exp. Biol.* **215**, 4055-4069.

Stoessel, A., Kilbourne, B.M., and Fischer, M.S. (2013). Morphological integration vs. ecological plasticity in the avian pelvic limb skeleton. *J. Morph.* **274**, 483-495.

Taylor, C.R., Heglund, N.C., McMahon, T.A., and Looney, T.R. (1980). Energetic cost of generating muscular force during running: a comparison of large and small animals. *J. Exp. Biol.* **86**, 9-18.

Taylor, C.R., Shkolnik, A., Dmi'el, R., Baharav, D., and Borut, A. (1974). Running in cheetahs, gazelles, and goats: energy cost and limb configuration. *Am. J. Physiol.* **227**, 848-850.

Umberger, B.R. (2010). Stance and swing phase costs in human walking. *J. R. Soc. Interface* **6**, 1329-1340.

van Coppenolle, I., and Aerts, P. (2004). Terrestrial locomotion in the white stork (*Ciconia ciconia*): spatio-temporal gait characteristics. *Anim. Biol.* **54**, 281-292.

Verstappen, M., Aerts, P., and Van Damme, R. (2000). Terrestrial locomotion in the black-billed magpie: kimematic analysis of walking and out-of-phase hopping. *J. Exp. Biol.* **203**, 2159-2170.

White, C.R., Martin, G.R., and Butler, P.J. (2008). Pedestrian locomotion energetics and gait characteristics of a diving bird, the great cormorant, *Phalacrocorax carbo*. *J. Comp. Physiol.* **178**, 745-754.

Wickler, S.J., Hoyt, D.F., Clayton, H.M., Mullineaux, D.R., Cogger, E.A., Sandoval, E., McGuire, and R., Lopez, C. (2004). Energetic and kinematic consequences of weighting the distal limb. *Equine Vet. J.* **36**, 772-777.

Wilson, A.M., Watson, J.C., and Lichtwark, G.A. (2003). A catapult action for rapid limb protraction. *Nature* **421**, 35-36.

Tables

Table 1. Body mass and number of analyzed strides for individual study animals. N_{Stride} denotes number of strides analyzed. Note that 5769 (1), 5769 (4), and Grün never fully acclimated to locomoting on the treadmill, leading to a paucity of data for these individuals. Asterisks denote individuals sacrificed to measure limb segment masses.

Individual	**Body Mass** (g)	$\mathbf{N_{Stride}}$
avocet		
Orange*	285.0	42
Silber	348.0	28
Grün	358.0	3
Weiß	344.0	19
oystercatcher		
5769 (1)	450.0	7
5769 (4)	490.0	1
3970 (5)*	433.3	86
3970 (7)	455.0	35
lapwing		
B65	169.8	24
B67	184.9	18
B76	163.2	29
B100*	163.6	29

Table 2. Hindlimb segmental properties of the three species studied. Values of segment mass and length slightly differ from Figure 1, as they are from a hitherto unpublished sister study on charadriiform locomotor kinetics and were used to calculate MOI of individual limb segments. MOI of individual segments was measured with respect to the proximal end of the segment's bone(s).

Element	Weight (g)	% of Total mass	Length (mm)	CoM position (% of total segment length)	MOI (g cm^2)
avocet					
Whole limb	17.4	0.089	233	-	1554.5
Thigh	5.2	0.03	33	0.364	7.1
Shank	6.6	0.039	103	0.35	45.8
Tars. Segment	2	0.012	82	0.5	11.2
Digits	1.8	0.011	3.9	0.385	2.0
oystercatcher					
Whole limb	32.4	0.075	201	-	1720.4
Thigh	15.7	0.036	43	0.419	37.0
Shank	12.1	0.028	88	0.284	62.0
Tars. Segment	2.3	0.005	52	0.558	5.2
Digits	2.1	0.005	35	0.429	2.0
lapwing					
Whole limb	11.3	0.063	159	-	441.8
Thigh	5.7	0.033	323	0.485	06.85
Shank	3.8	0.022	65	0.33	11.5
Tars. Segment	0.9	0.005	446	0.5[c]	01.6
Digits	0.9	0.005	37	0.5[c]	1.0

Table 3. Power functions describing temporal kinematic traits as they vary with speed. Sample sizes for avocets, oystercatcers, and lapwings are N = 98, 129, and 99, respectively. Functions are in the form of $Y = a*Speed^b$.

	Absolute Speed		Dimensionless Speed	
Species	**a**	**b**	**a**	**b**
Stride Frequency				
Avocet	2.45 (2.419, 2.481)	0.43 (0.399, 0.461)	2.69 (2.653, 2.733)	0.22 (0.210, 0.241)
Oystercatcher	3.10 (3.065, 3.127)	0.54 (0.526, 0.561)	3.24 (3.217, 3.277)	0.27 (0.258, 0.275)
Lapwing	3.21 (3.168, 3.258)	0.41 (0.384, 0.435)	3.36 (3.310, 3.407)	0.20(0.191, 0.217)
Duty Factor				
Avocet	0.56 (0.553, 0.567)	-0.29 (-0.314, -0.269)	0.53 (0.518, 0.535)	-0.15 (-0.159, -0.135)
Oystercatcher	0.56 (0.553, 0.570)	-0.25 (-0.268, -0.227)	0.549 (0.541, 0.558)	-0.12 (-0.132, -0.112)
Lapwing	0.51 (0.504, 0.523)	-0.22 (-0.238, -0.209)	0.50, (0.491, 0.511)	-0.11 (-0.119, -0.105)
Swing Duration				
Avocet	0.18 (0.173, 0.183)	0.04 (-0.018, 0.097)	0.18 (0.173, 0.186)	0.02 (-0.012, 0.046)
Oystercatcher	0.14 (0.134, 0.141)	-0.19 (-0.229, -0.150)	0.135 (0.131, 0.139)	-0.09 (-0.113, -0.074)
Lapwing	0.14 (0.146, 0.154)	0.05 (0.020, 0.081)	0.15 (0.147, 0.155)	0.03 (0.010, 0.040)
Stance Duration				
Avocet	0.23 (0.227, 0.240)	-0.69 (-0.726, -0.645)	0.20 (0.196, 0.211)	-0.34 (-0.364, -0.322)
Oystercatcher	0.18 (0.174, 0.182)	-0.88 (-0.899, -0.854)	0.164 (0.160, 0.168)	-0.43 (-0.445, -0.422)
Lapwing	0.15 (0.147, 0.162)	-0.71 (-0.732, -0.691)	0.14 (0.133, 0.149)	-0.36 (-0.370, -0.347)

Table 4. Comparison of the masses of limb segment and their corresponding limb bones. 'Difference' is the estimate of soft tissues comprising each segment, calculated as the difference between segment and bone mass. Segment mass and limb bone data are from separate adult individuals, and therefore should be considered to offer a rough estimate in how these three species differ in the amount that soft tissues contribute to segment mass. Values are in grams.

Species	Segment	Bone	Difference
Avocet[1]			
Thigh	5.20	0.37	4.83
Shank	7.30	1.18	6.12
Tars. Segment	2.57	0.84	1.73
Oystercatcher[2]			
Thigh	15.74	0.81	14.93
Shank	10.96	1.22	9.74
Tars. Segment	2.3	0.67	1.63
Lapwing[3]			
Thigh	5.14	0.32	4.82
Shank	4.03	0.53	3.5
Tars. Segment	0.87	0.27	0.6

Specimens used to measure bone mass: [1]Zoologisches Museum Berlin (ZMB) Aves 83/17; [2]ZMB Aves 75.116 and ZMB Aves 68.16; [3]ZMB Aves 68.181 and ZMB Aves 68.125

Figures

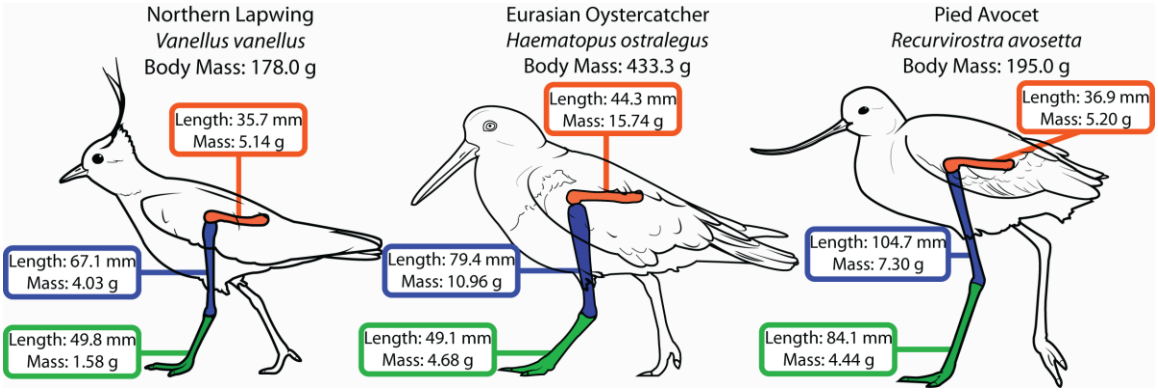

Figure 1. **Comparison of limb proportions in charadriiform species sampled in our study**. Orange denotes the femur length and thigh segment mass, blue denotes the tibiotarsus length and shank segment mass, and green denotes the tarsometatarsus length and pes mass (inclusive of the digits). Specimens used to measure bone length were Zoologischer Museum Berlin (ZMB) Aves 83/17 (pied avocet); ZMB Aves 75.116 and ZMB Aves 68.16 (Eurasian oystercatcher); and ZMB Aves 68.181 and ZMB Aves 68.125 (northern lapwing). For methodology of dissecting hindlimb segments, see Kilbourne (2014).

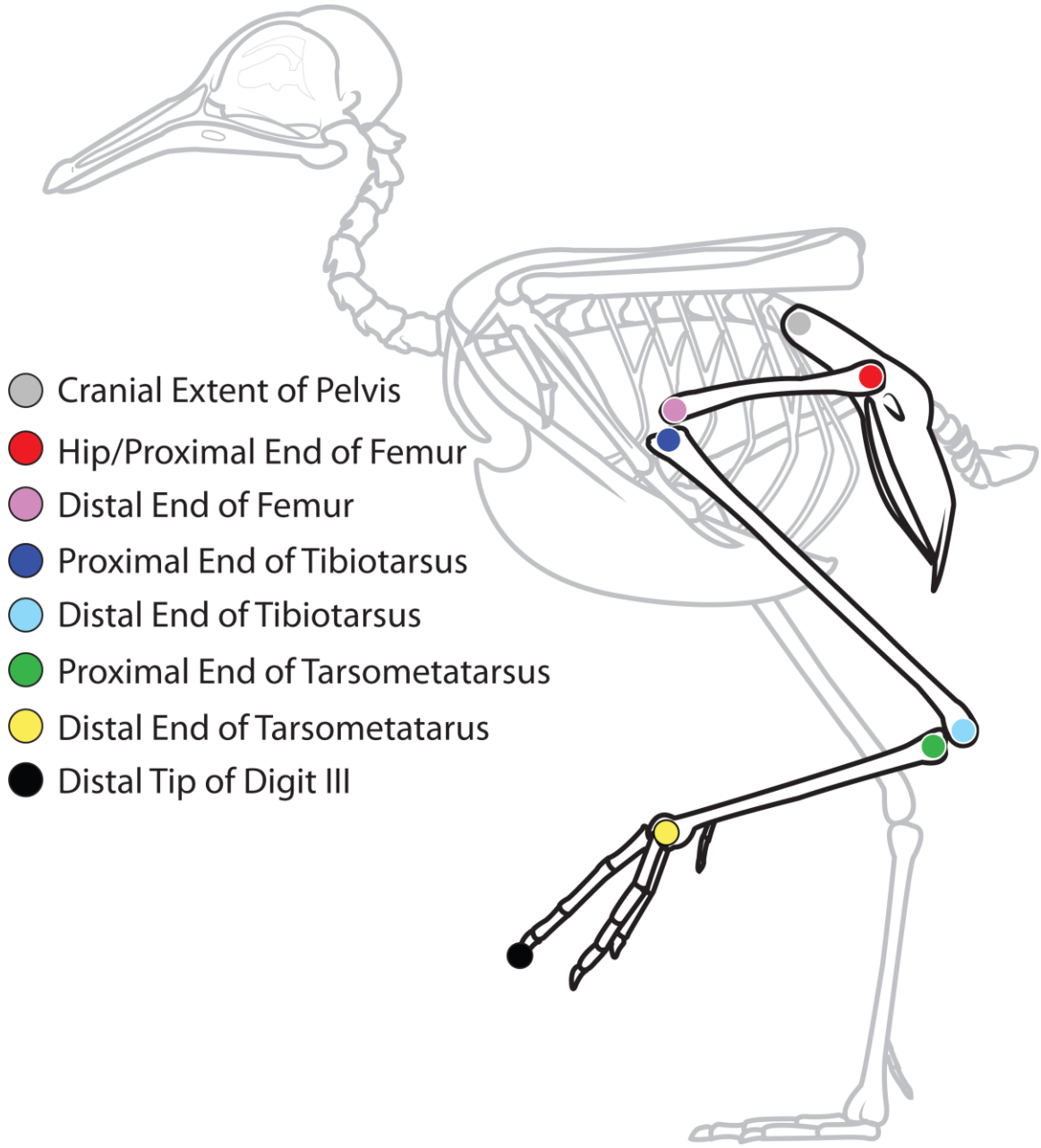

Figure 2. **Skeletal landmarks and joints used to study hindlimb kinematics**. Bones with digitized landmarks are outlined in black; other bones are outlined in grey.

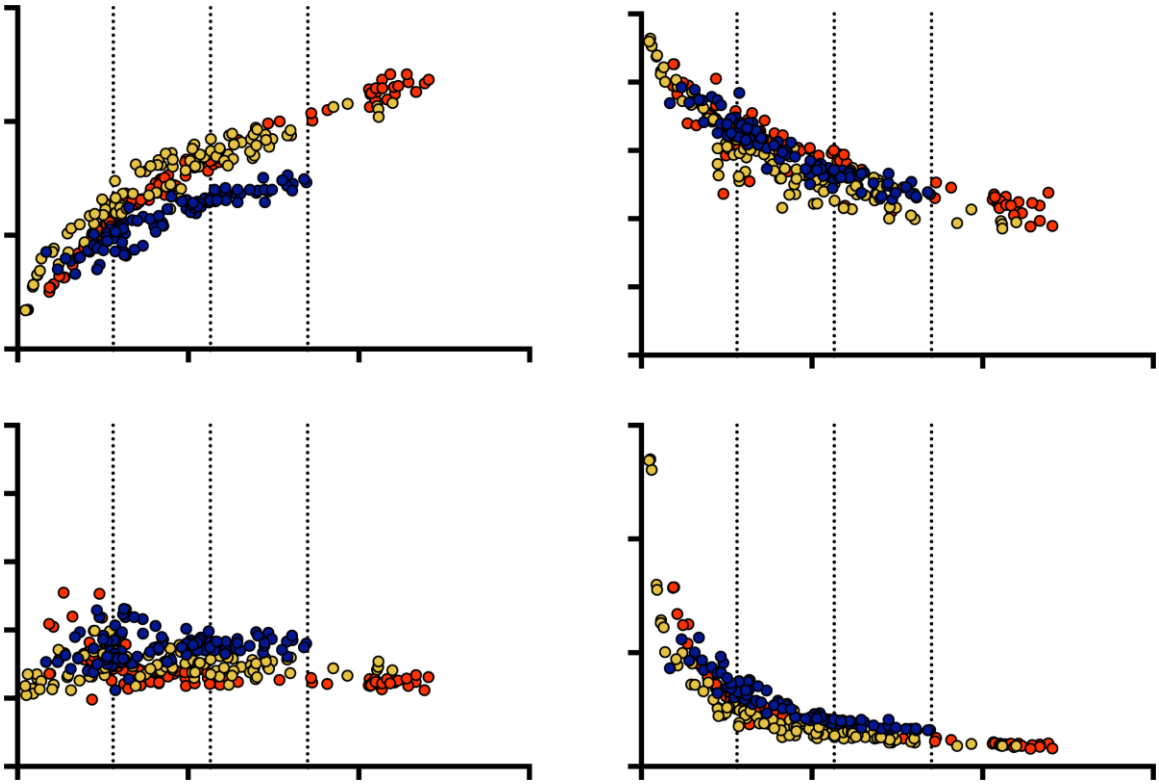

Figure 3. **Temporal parameters of hindlimb kinematics as a function of absolute speed**. Stride frequency (A), duty factor (B), and swing (C) and stance durations (D) are all plotted against speed. Data for oystercatchers, lapwings, and avocets are plotted in red, yellow, and blue, respectively. 'L,' 'M,' and 'H' respectively denote low, middle, and high speed categories.

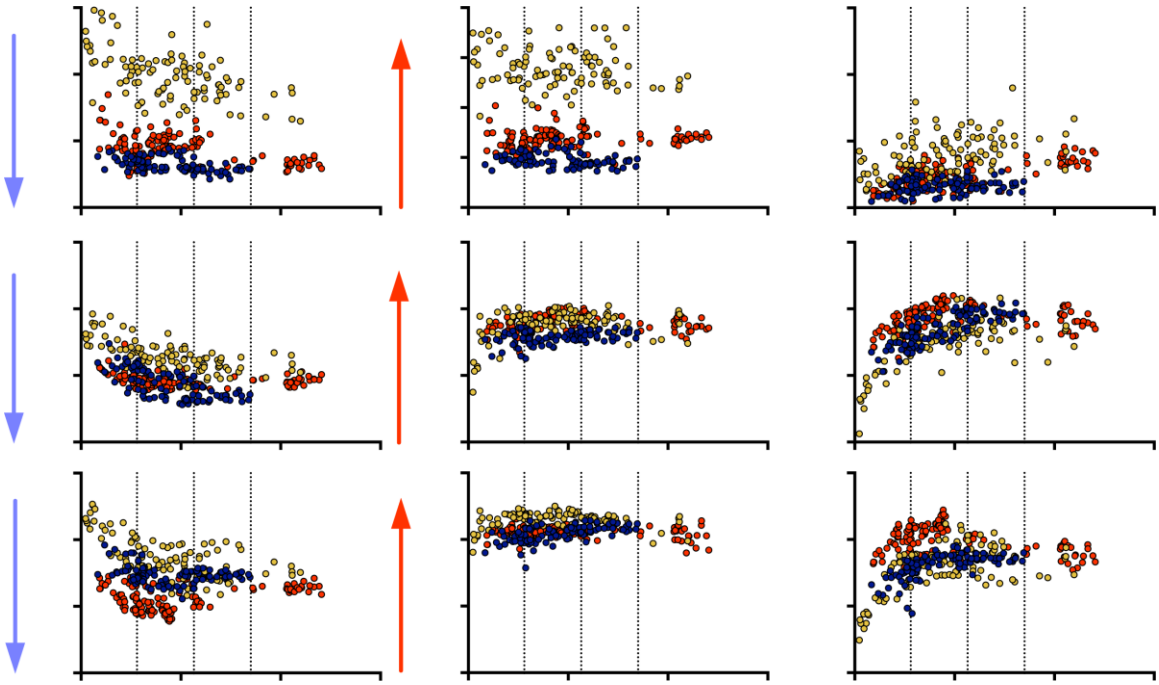

Figure 4. Maximum joint flexion, extension, and ranges of motion during swing phase as a function of absolute speed. Hip kinematics are plotted in A to C, knee kinematics are plotted in D to F, and intertarsal joint kinematics are plotted in G to I. Blue arrows denote the direction of increasing flexion, whereas red arrows denote the direction of increasing extension. Data for oystercatchers, lapwings, and avocets are plotted in red, yellow, and blue, respectively. L,' 'M,' and 'H' respectively denote low, middle, and high speed categories.

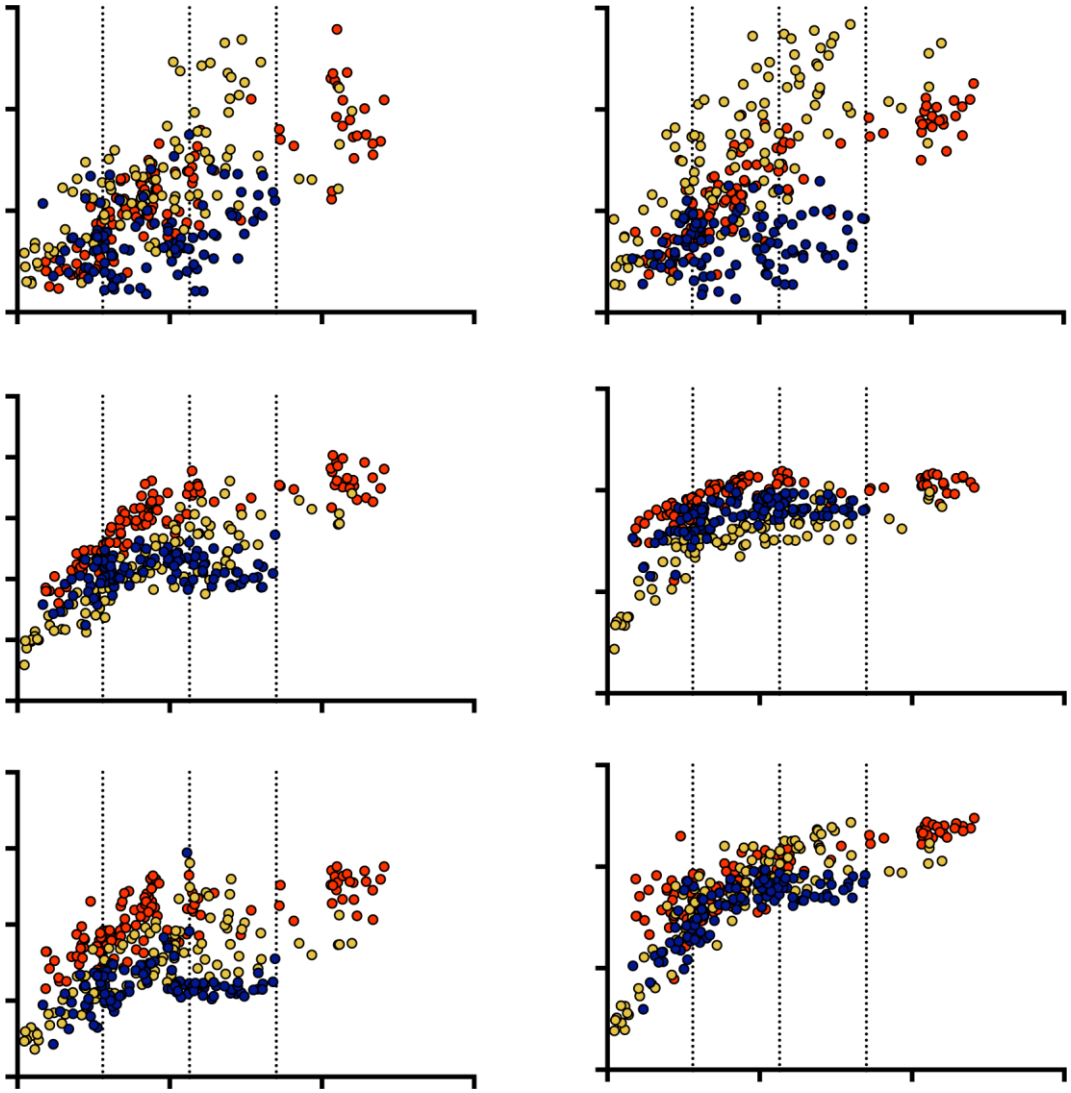

Figure 5. **Maximum angular velocities and excursions of hindlimb segments during swing phase as a function of absolute speed**. Velocities and excursions of the thigh, shank, and pes are shown in A and B, C and D, and E and F, respectively. Data for oystercatchers, lapwings, and avocets are plotted in red, yellow, and blue, respectively. L,' 'M,' and 'H' respectively denote low, middle, and high speed categories.

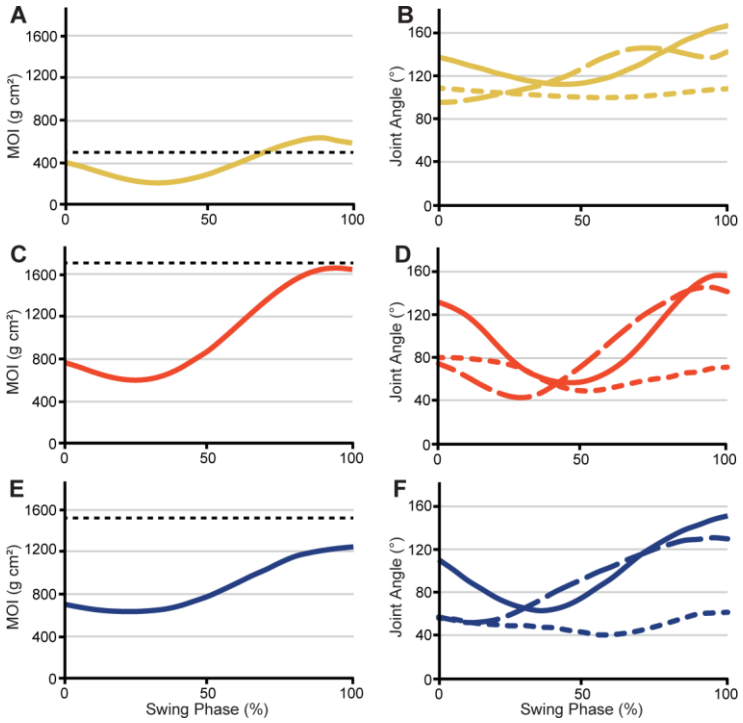

Figure 6: MOI and limb joint kinematics over the duration of swing phase. Data for oystercatchers, lapwings, and avocets are plotted in red, yellow, and blue, respectively. Black dashed lines in A, C, and E represent 'neutral pose' MOI published in Kilbourne, 2013. Dotted lines in B, D, and F represent the hip joint. Dashed lines in B, D, and F represent the knee joint. Solid lines in B, D, and F represent the intertarsal joint. Representative trials of lapwing, oystercatcher and avocet at 0.84 m/sec; 1.19 m/sec, and 0.83 m/sec, respectively.

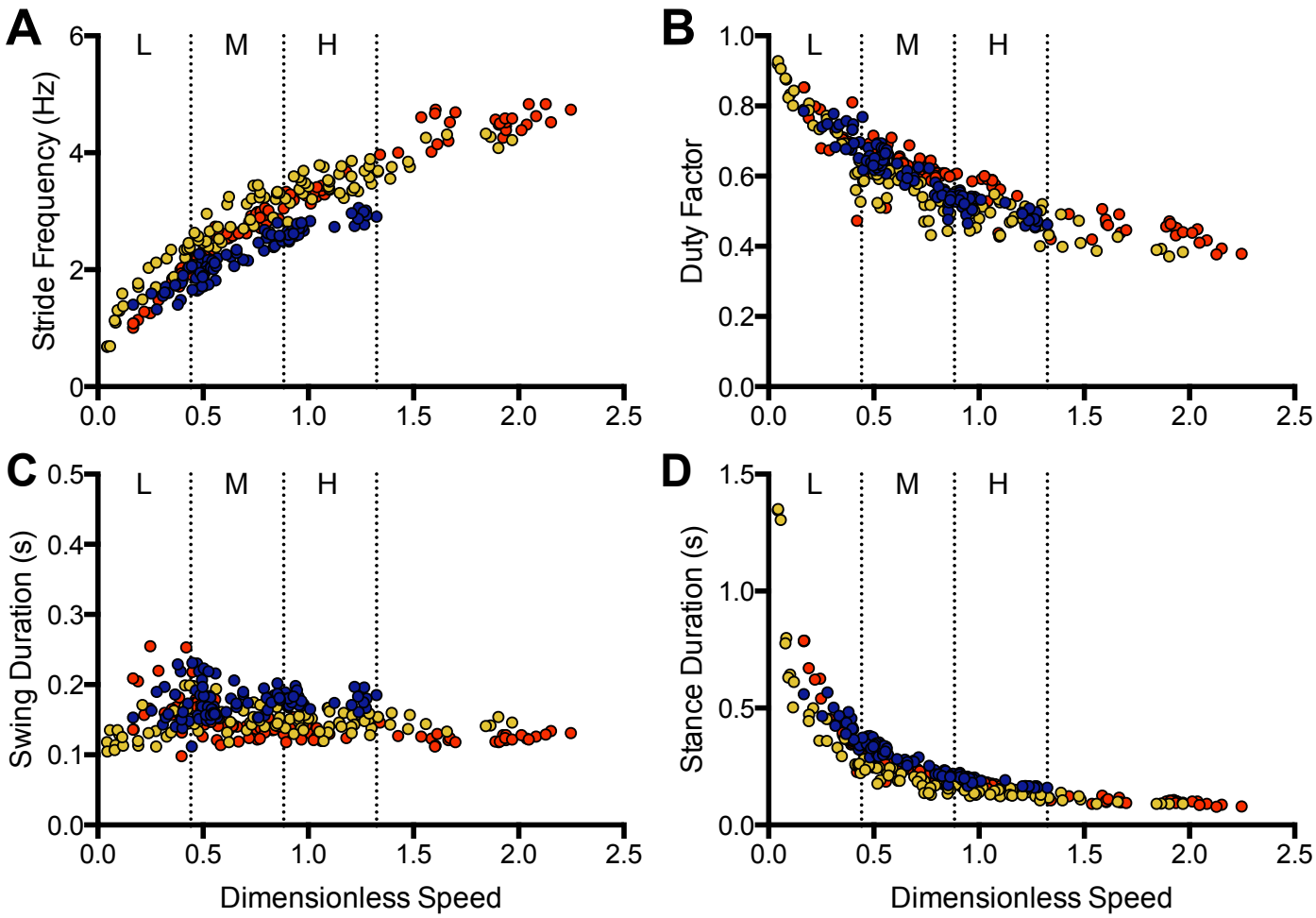

Fig. S1. Temporal parameters of hindlimb kinematics vs. dimensionless speed. Stride frequency (A), duty factor (B), and swing (C) and stance durations (D) are all plotted against speed. Data for oystercatchers, lapwings, and avocets are plotted in red, yellow, and blue, respectively. 'L,' 'M,' and 'H' respectively denote low, middle, and high speed categories.

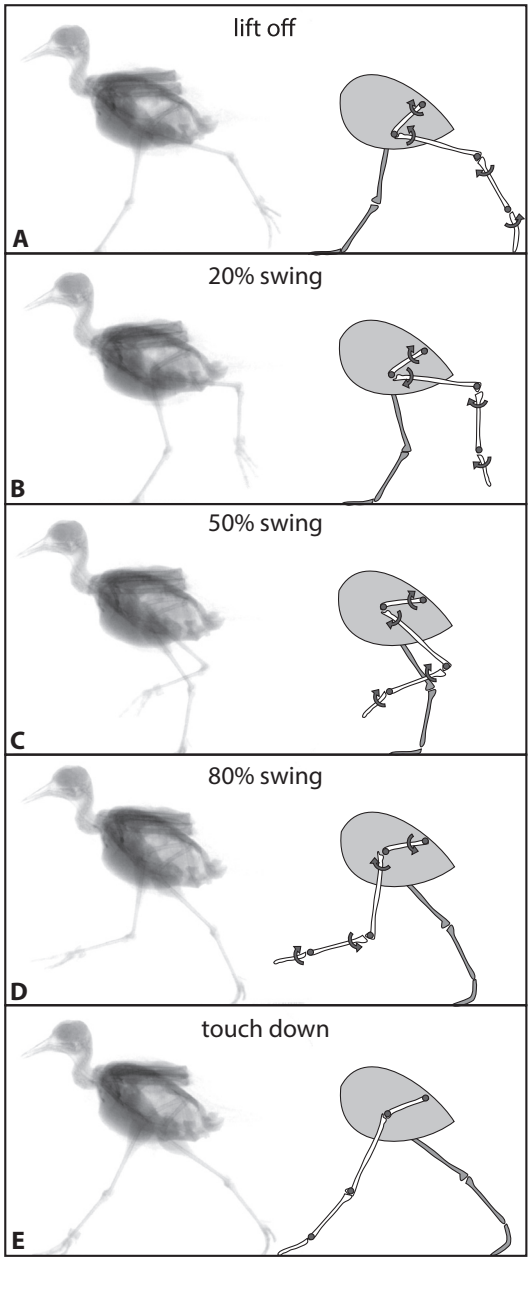

Fig. S2: Representative x-ray stills and schematic drawings of the swing phase during a grounded run of a Northern lapwing. Arrows indicate segmental movement. Note that not all limb segments are rotated in the direction of movement at all times during swing. Initially, the knee undergoes flexion (A) before it extends throughout the rest of swing phase, at mid-swing (C) all segments are protracted, and well before touch down (D, E) the hip and intertarsal joint start to extend.

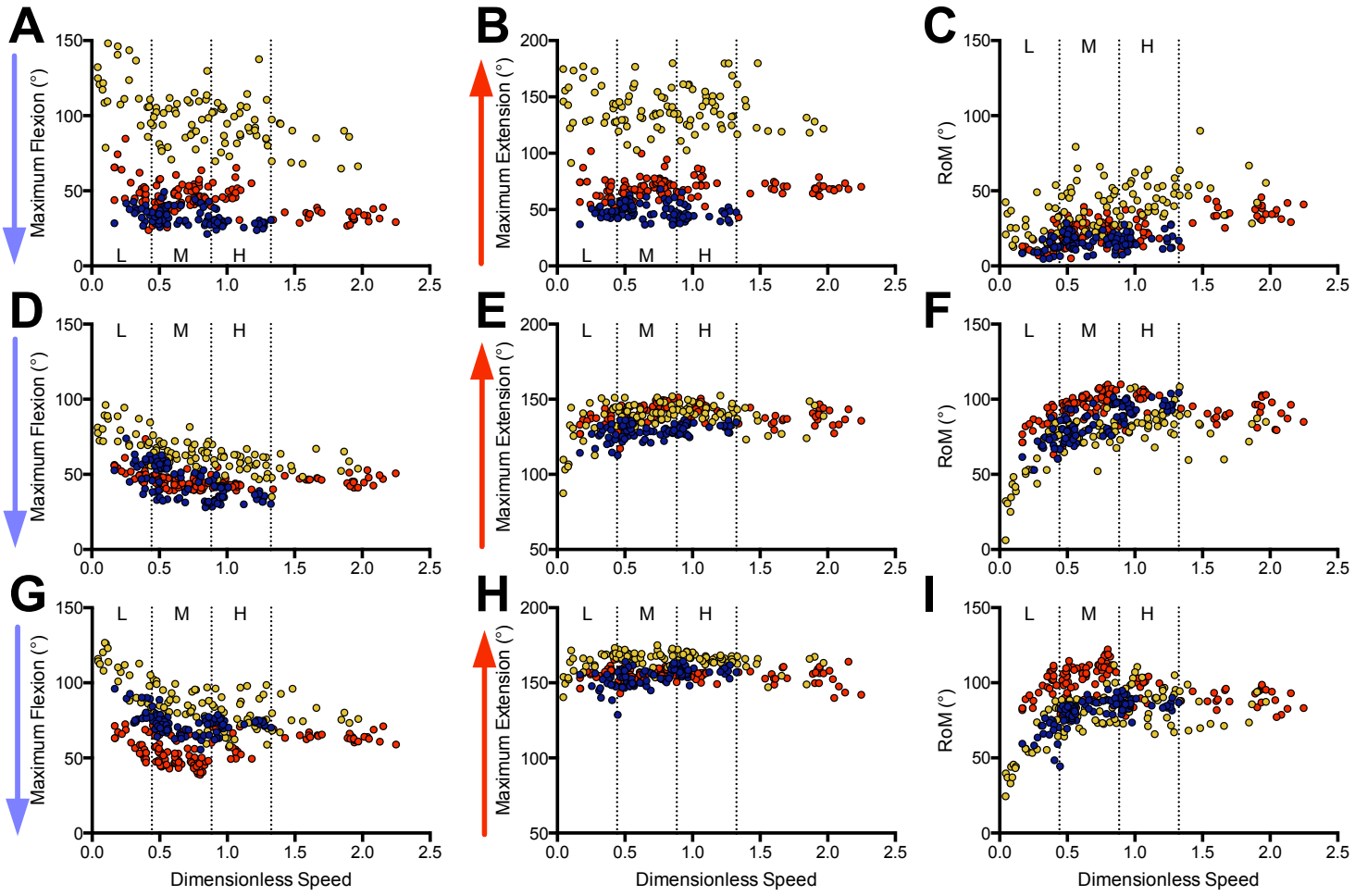

Fig. S3. Maximum joint f exion, extension, and ranges of motion during swing phase as a function of dimensionless speed. Hip kinematics are plotted in A to C, knee kinematics are plotted in D to F, and intertarsal joint kinematics are plotted in G to I. Blue arrows denote the direction of increasing flexion, whereas red arrows denote the direction of increasing extension. Data for oystercatchers, lapwings, and avocets are plotted in red, yellow, and blue, respectively. L,' 'M,' and 'H' respectively denote low, middle, and high speed categories.

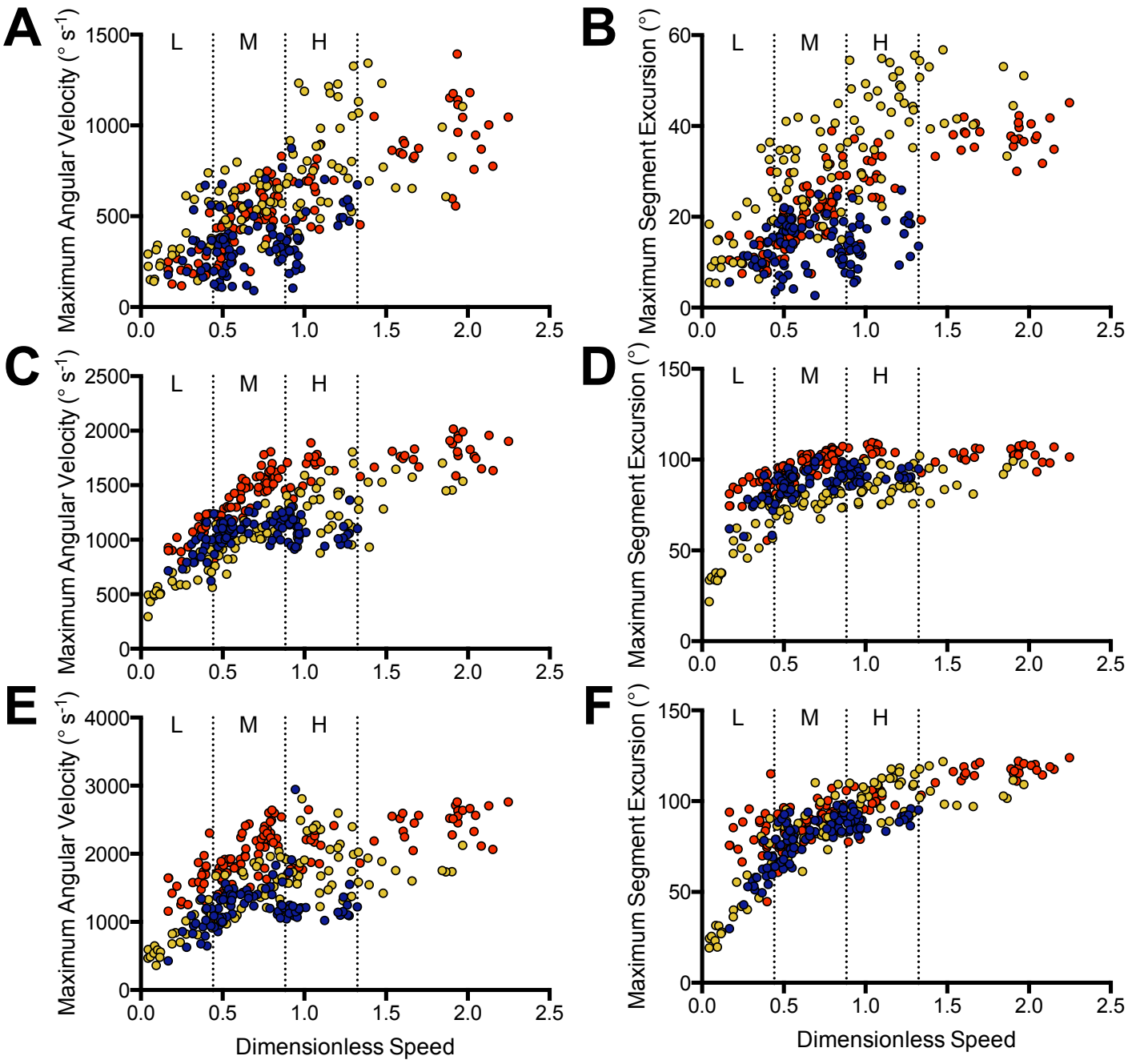

Fig. S4. Maximum angular velocities and excursions of hindlimb segments during swing phase as a function of dimensionless speed. Velocities and excursions of the thigh, shank, and pes are shown in A and B, C and D, and E and F, respectively. Data for oystercatchers, lapwings, and avocets are plotted in red, yellow, and blue, respectively. L,' 'M,' and 'H' respectively denote low, middle, and high speed categories.

Table S1. Avocet speed, temporal, and joint angle raw data

Click here to Download Table S1

Table S2. Oystercatcher speed, temporal, and joit angle raw data

Click here to Download Table S2

Table S3. Lapwing speed, temporal, and joint angle raw data

Click here to Download Table S3

Table S4. AICc scores indicating relative quality of fit of linear and power functions to temporal kinematic parameters as they vary with speed. Scores for the better fitting function are highlighted in bold.

	Absolute Speed		Dimensionless Speed	
Parameter	Linear Fit	Power Fit	Linear Fit	Power Fit
Stride Frequency				
Avocets	-80.4	**-99.2**	-36.8	**-107.2**
Oystercatcher	-1.1	**-149.7**	153.3	**-101.9**
Lapwings	-8.9	**-116.7**	159.7	**-17.6**
Duty Factor				
Avocets	-397.8	**-403.1**	-340.7	**-386.1**
Oystercatchers	-429-5	**-441.2**	-380.1	**-436.9**
Lapwings	-251.3	**-326.8**		
Swing Duration				
Avocets	-468.2	**-468.7**	-466.7	**-467.5**
Oystercatchers	-623.8	**-643.8**	-607.0	**-643.8**
Lapwings	-496.6	**-505.9**	-494.2	**-505.9**
Stance Duration				
Avocets	-346.5	**-414.2**	-291.4	**-403.6**
Oystercatchers	-246.8	**-625.5**	-204.8	**-622.0**
Lapwings	-57.7	**-369.2**	-25.2	**-350.9**